Journal of Soil Contamination, 5(1): (1996)

The Effect of Interfacial Tension on Hydrocarbon Entrapment and Mobilization Near a Dynamic Water Table

Robert G. Ryan and V. K. Dhir

Department of Mechanical, Aerospace, and Nuclear Engineering, University of California, Los Angeles, CA 90024

ABSTRACT: The entrapment of residual hydrocarbon ganglia during water table fluctuations can produce a long-term contamination threat to groundwater supplies that is difficult to remove. The mobilization of entrapped hydrocarbon ganglia depends on the balance between capillary and gravitational forces represented by the Bond number. The present work focuses on the influence of the interfacial tension between the hydrocarbon and the surrounding water on the entrapment and mobilization of the residual ganglia. Laboratory column tests using glass beads as the porous medium have been conducted to determine the residual saturation of a hydrocarbon (Soltrol 170) trapped during vertical displacements due to a rising water table and the necessary decrease in interfacial tension to mobilize these trapped ganglia. The interfacial tension was decreased by the addition of isopropyl alcohol to the water phase. Saturations of the three phases (water, hydrocarbon, and air) were measured with a dual-beam γ-densitometer. The results for residual hydrocarbon saturation at various interfacial tensions were combined with previous results for different particle diameters to provide a general relationship between residual saturation and Bond number. The relationship is expressed in an empirical correlation valid for Bond numbers between 0.001 and 1.2.

KEY WORDS: petroleum hydrocarbons, groundwater contamination, soil contamination.

I. INTRODUCTION

Petroleum products can present a significant source of groundwater contamination following accidental spills or leaks from aging underground tanks. Liquid hydrocarbons are often referred to as LNAPLs (light nonaqueous-phase liquids) because they are generally immiscible with water and have a specific gravity less than one.

Small LNAPL discharges into soil will usually not reach the water table, but will migrate downward and laterally under the influence of gravity and capillary forces until the LNAPL becomes discontinuous and immobile. However, a plume from a large LNAPL spill can reach the water table where, due to its lighter density, it

will spread laterally as shown in Figure 1. The water table will be locally depressed near the center of the plume, but will recover as the plume continues to spread over the capillary fringe. As the water table returns to its original level, some of the LNAPL will become trapped as it is vertically displaced, forming an immiscible lens of water and contaminant. Similar regions of residual LNAPL can be created anywhere the plume contacts the capillary fringe due to seasonal fluctuations in the water table. Due to its location in the saturated zone and its large interfacial area in contact with the water phase, this residual LNAPL is especially dangerous to groundwater quality. The effect of contaminant distribution in the capillary fringe and saturated zones on groundwater remediation efforts has been well described by Hoag *et al*. (1991).

The static distribution of fluids in porous media was originally studied by Leverett (1941). A correlation between capillary pressure and saturation was developed from experimental results using clean sands as the media and water and air as the fluids. Hysteresis between the results for drainage and imbibition was clearly shown.

In order to establish a correlation for three-fluid systems (e.g., water, LNAPL, and air), Lenhard and Parker (1988) developed a three-phase retention cell to

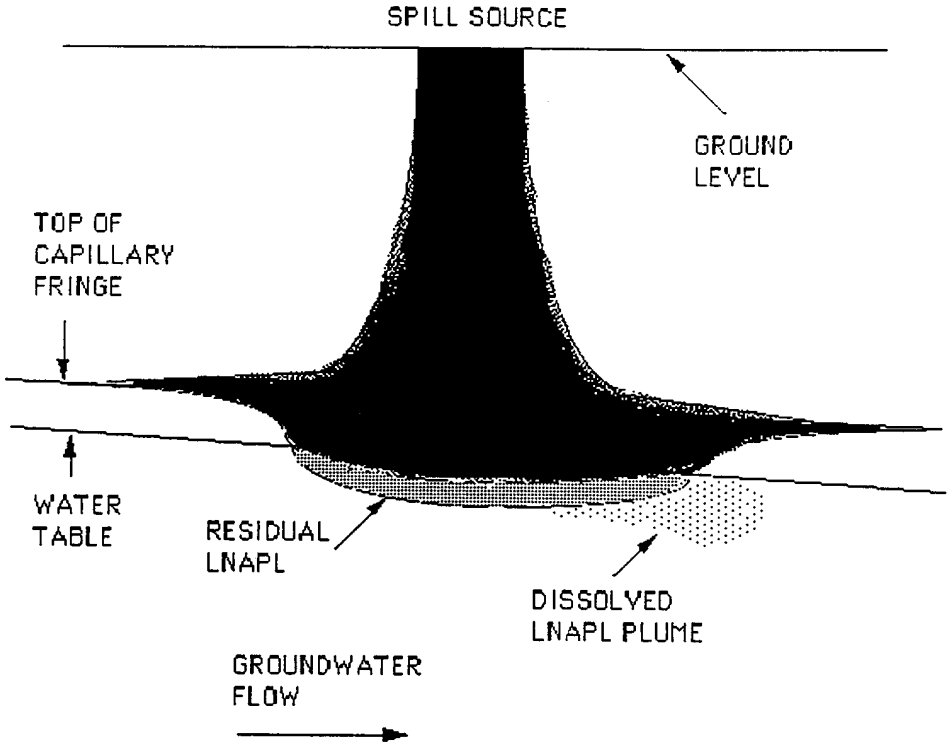

FIGURE 1. Interaction of LNAPL spill with water table.

simultaneously measure the pressures of the water and LNAPL phases. Their results indicated that Leverett's (1941) correlation could be extended to three fluids, with the assumption that the order of wettability is water, LNAPL, air. Parker and Lenhard (1987) noted the complexity of hysteresis in three-fluid systems due to the greater number of possible path directions. Their model used water-air drainage saturation data to develop a pore-size distribution for the porous medium, based on fitted parameters describing the saturation profile. Using these parameters and residual saturation data from two-fluid experiments, three-fluid saturation profiles were predicted for any path direction. The LNAPL phase was assumed to exist continuously or as discontinuous globules or ganglia. Numerical simulations of LNAPL entrapment due to water table fluctuations were reported by Lenhard *et al*. (1989). Experimental measurements of LNAPL entrapment in an unconsolidated sandy medium were performed by Lenhard *et al* (1993).

A more detailed model for residual NAPL mobilization has been proposed by Dawson (1992). Starting from a force balance on a NAPL ganglion, expressions were developed for NAPL residual saturation as a function of dimensionless parameters describing the importance of viscous, buoyancy, and capillary forces (i.e., capillary number and Bond number). Additional parameters of importance in this model are the relative permeability to water at residual LNAPL saturation conditions, the average ganglion length, and a factor to scale static equilibrium capillary pressures to dynamic equilibrium capillary pressures. According to simulations presented for trichloroethylene (TCE), the average ganglion length is on the order of tens of centimeters.

Mobilization of residual oil by water flooding has been studied extensively due to its importance to the petroleum industry. It has generally been noted that significant mobilization of residual oil occurs at a particular value of capillary number, which represents the ratio of viscous forces to capillary forces. The capillary number can be expressed as:

$$N_{ca} = k\Delta P / L\sigma = q\mu / \sigma \quad (1)$$

where k permeability of the porous medium
$\Delta P / L$ viscous pressure gradient
σ interfacial tension between water and oil
μ dynamic viscosity of water
q specific discharge of the water

For low water flow rates where buoyancy forces are no longer negligible, a Bond number is introduced that represents the ratio of buoyancy forces to capillary forces. A mobility number that accounts for the influence of viscous, buoyancy, and capillary forces was defined by Boyd and Farley (1992) as:

$$N_{mo} = (N_{ca} + k_{rw}N_{Bo}) / \varepsilon \quad (2)$$

where k_{rw} relative permeability to water
N_{Bo} Bond number = $k\Delta\rho g \sin \alpha / \sigma$
$\Delta\rho$ density difference between water and NAPL
α angle between column and horizontal plane
g acceleration of gravity
ε porosity

A series of laboratory column experiments by Ryan and Dhir (1993) examined the effect of particle diameter on LNAPL entrapment by a slowly rising water table. Soltrol 170 was used as the LNAPL. The LNAPL was added at the top of a 3-in. i.d. plexiglass column and allowed to infiltrate through the test section. Subsequently, water was added at the base of the column until the free LNAPL was displaced out of the test section. Water and residual LNAPL saturations at several vertical locations in the test section were measured using a dual-beam γ-densitometer. Tests were run with glass bead packs of diameters ranging from 210 to 6000 μm and a representative soil (Synthetic Soil Matrix, available from Foster Wheeler Enviresponse, Inc., Edison, NJ). The LNAPL saturation trapped by the displacement by water was related to a Bond number based on particle diameter (rather than permeability), defined as:

$$Bo = \Delta\rho g D_p^2 / \sigma \quad (3)$$

where D_p is the particle diameter.

The results led to several conclusions:

1. The amount of LNAPL trapped was different if the particles were initially wetted with water prior to LNAPL addition. Bead packings that were dry prior to LNAPL addition trapped a negligible amount of LNAPL, which is attributed to the effect of the contact angle on the "snap-off" trapping mechanism, illustrated in Figure 2. When an LNAPL ganglion is displaced through the pore space, the advancing water can wet the pore neck (at r_n) and cause the water/LNAPL interface at the neck to collapse, leaving a blob of LNAPL trapped in the pore belly. This effect is enhanced for a low contact angle (measured through the water phase) and large values of aspect ratio (r_b/r_n). Bead packings that were a mixture of "water-wet" and "water-dry" particles trapped a large amount of LNAPL, believed to be due to "fingering" of the displacing water caused by the spatial variation of contact angle (Ryan, 1994).
2. Bead packings that were initially wetted with water were considered to be representative of natural conditions in an aquifer. For these bead packings, the residual LNAPL saturation was found to be quite uniform and not sensitive to the initial amount of water saturation. For particle sizes of

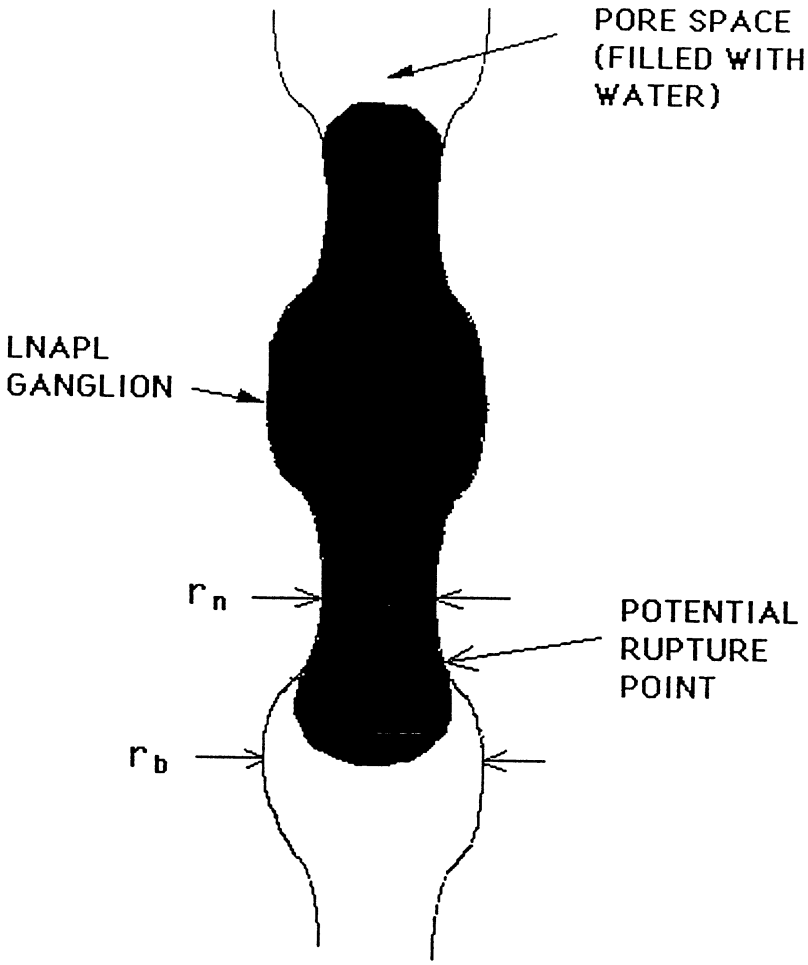

FIGURE 2. Illustration of "snap-off" mechanism with water as the wetting fluid.

710 μm and below, there was no discernible effect of particle diameter and the average residual LNAPL saturation was 11%. Larger particle sizes produced lower levels of residual LNAPL, with no measurable trapping for 6000-μm particles.

3. The synthetic soil matrix (SSM) trapped a similar amount of contaminant as the glass beads, with an average residual saturation of 10.9%. This is somewhat expected, as approximately half of the soil particles in the SSM were smaller than 710 μm (overall, the range was from 45 μm to 6400 μm). It might be expected that the large deviation in particle sizes (and presum-

ably, pore sizes) would have a noticeable effect on contaminant trapping, but this was not observed.

The present work seeks to establish a correlation between residual LNAPL saturation in the saturated zone and Bond number by analyzing column experiments conducted with a range of interfacial tension values between the water and the LNAPL phases.

II. EXPERIMENTAL PROCEDURE

The experimental apparatus used was similar to that described in Ryan and Dhir (1993). A test section for the LNAPL displacement measurements was constructed from a 9-in.-long segment of 3-in. i.d. plexiglass tubing with a 1/4" wall thickness. Several probes were installed in the wall of the test section to allow air to escape when LNAPL was added at the top of the column. A fine stainless steel screen was used at the bottom of the test section to hold the glass particles in place. The screen was made by glueing a section of screen material to a 1/4-in.-long piece of 3-in. ABS pipe. Two 3-in. "no-hub" rubber couplings with hose clamps were used to hold the screen in place and connect the test section with the adjacent plumbing. Above the test section is another piece of plexiglass tubing so that displaced LNAPL can be observed and removed for volume measurement. A 3-in. ABS Y-fitting was used as a base for the vertical segment in which the test section was mounted, and connects to a supply tank through a combination of PVC pipe and plastic tubing. The height of the supply tank can be varied to simulate changes in water table height. A rotameter and a needle valve are installed in the connecting tubing to allow for flow rate measurement and control. Figure 3 shows the arrangement of the apparatus.

A dual-beam γ-densitometer was used to measure the *in situ* saturations of water and LNAPL at six vertical locations in the test section. An important advantage of this technique is the ability to measure the spatial distribution of the trapped LNAPL throughout the test section. The instrument consists of two γ- sources (cesium and americium) and a sodium-iodide detector, both encased in lead and mounted on a lift truck for easy height adjustment. A schematic showing the relative positions of the γ- sources, the detector, and the test section is shown in Figure 4. The calculation of the fluid saturations is based on the exponential relationship between γ-beam attenuation and the thickness of the attenuating medium. For a test section filled with a porous medium partially saturated with two liquids (denoted by subscripts 1 and 2), this relationship can be written as:

$$I_i = I_{oi} \exp(-\mu_{1i} X S_1 \varepsilon - \mu_{2i} X S_2 \varepsilon) \quad (4)$$

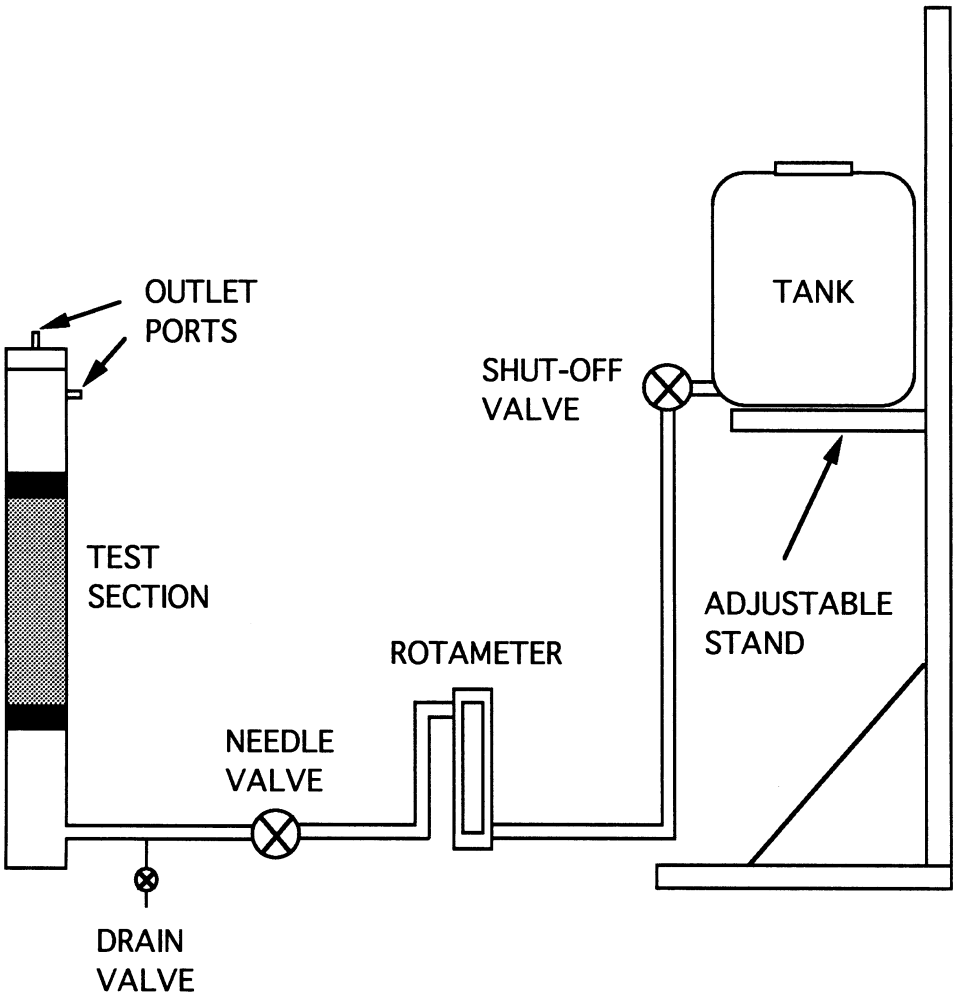

FIGURE 3. Test apparatus schematic.

where I_o count rate through the dry medium
I count rate through the partially saturated medium
μ γ-attenuation coefficient of the liquid
X thickness of the porous medium
S saturation (i.e., the fraction of the pore space filled with liquid)
ε porosity
i index denoting the gamma source

Because there are two unknowns in the attenuation relationship (S_1 and S_2), the two beams provide the necessary two equations. The inherent uncertainties in satura-

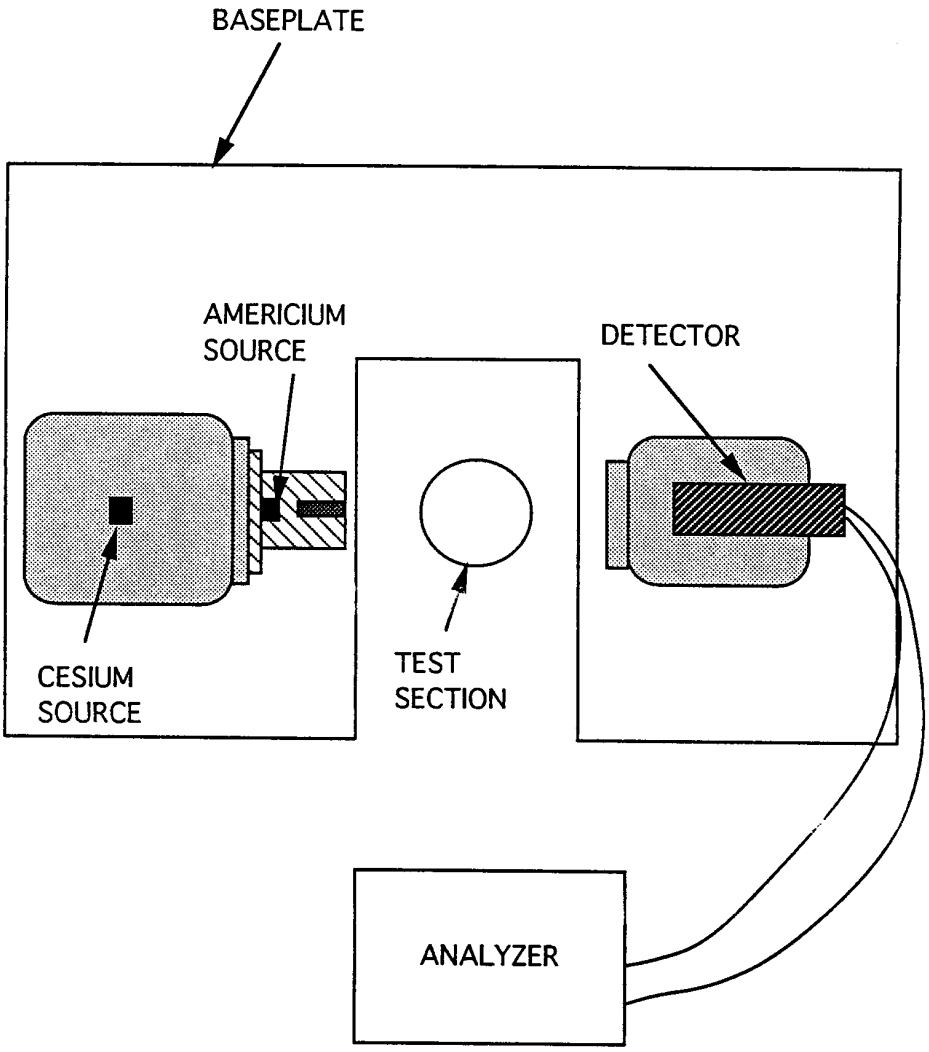

FIGURE 4. Densitometer schematic.

tion values calculated from this ill-conditioned pair of equations is minimized by adding doping agents to the water (sodium bromide) and LNAPL (iodoheptane) that change the fluids' γ-attenuation coefficients. Additional information on the γ-densitometer and a detailed error analysis are discussed in Ryan (1994).

The addition of isopropyl alcohol to the water/LNAPL system provided a means to decrease the interfacial tension between the water and the LNAPL phases. The "drop-weight" method (Adamson, 1967) was used to measure interfacial tensions. Some preliminary measurements were performed to establish the attainable variation in interfacial tension; the results are shown in Figure 5. A reduction in

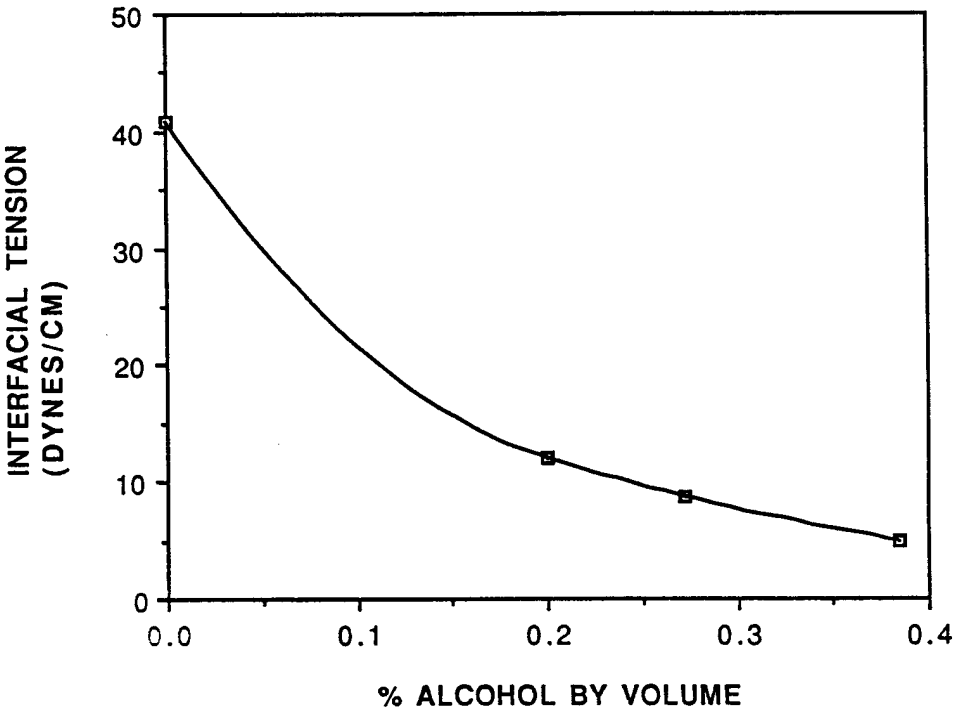

FIGURE 5. Effect of isopropyl alcohol addition on interfacial tension between water and LNAPL.

interfacial tension by a factor of approximately eight (from 40.9 to 4.9 dyn/cm) was measurable by the drop-weight technique using a standard eyedropper, which was sufficient for the experimental objectives.

Prior to the addition of porous material to the test section, 5-min densitometer counts were collected at each of the six measurement locations, which allowed for the determination of local porosity (Ryan and Dhir, 1993). Local porosity values ranged from 37 to 41%. These values compared well with bulk porosities found from packing particles in graduated cylinders partially filled with water, and noting the volumes of the porous medium and the displaced water. The densitometer counts were repeated after the glass particles were added (which gives I_o in the attenuation equation).

Two types of displacement experiments were performed. In the first type (type 1), the supply tank was filled with a mixture of water, sodium bromide (NaBr), and alcohol. (This mixture is subsequently referred to as the water/alcohol phase.) Sufficient alcohol was added to reduce the interfacial tension by approximately five times. The supply valve was then opened so that this mixture infiltrated the entire test section. Subsequently, the supply valve was closed and a drain valve was used to drain the test section until only the bottom portion appeared to be fully

saturated. The initial saturation profile created by this procedure was then measured with the densitometer. Next, approximately 200 ml of LNAPL (Soltrol 170 mixed with iodoheptane) was added at the top of the test section, and after equilibrium conditions were reached, the saturation profiles were measured again.

Displacement of the LNAPL was accomplished by opening the supply valve and allowing the water/alcohol phase in the supply tank to enter the base of the column at a rate of approximately 5 ml/min (corresponding to a capillary number of 4.4E-7). This flow was continued until the displaced LNAPL was visible above the test section, where the thickness of the layer (and thus the volume) was noted. The saturation profiles in the test section were then measured with the densitometer. A second cycle of lowering and raising the water level followed (with the displaced LNAPL being allowed to reenter the test section), and the saturation profiles were again measured with the densitometer. Finally, samples of the water/alcohol and LNAPL phases were removed from the apparatus to measure the γ-attenuation coefficients and the interfacial tension. Type 1 tests were performed with 360- and 1500-μm particles. The chief purpose of these tests was to check for consistency with the results of Ryan and Dhir (1993), which were performed without alcohol addition.

The second series of tests (type 2) was designed to see if reductions in interfacial tension (and corresponding increase of Bond number) could mobilize LNAPL ganglia that were trapped at a lower Bond number. Type 2 tests were started by using the type 1 procedure described above, except that the supply tank was filled with water/NaBr (without alcohol). After the LNAPL was trapped by the displacement by water, alcohol was added to the supply tank and the supply flow was continued until the alcohol was distributed throughout the test section. The alcohol's ability to migrate through the water and air phases gives confidence that the concentration of the water/alcohol mixture in the test section will be uniform. Also, a fitting and drain tube were added to the top of the apparatus so that the water/alcohol phase could be recirculated while maintaining the free surface of the water/alcohol in the 3-in. plexiglass exit tube at a constant level (which allowed the mobilized LNAPL to be collected and measured). Saturation measurements were taken with the densitometer, and fluid samples were withdrawn to measure γ-coefficients and interfacial tension. If appropriate, additional alcohol could be added and the measurements repeated. Type 2 tests were conducted with 1500- and 3000-μm particles.

One of the experimental difficulties present in the type 2 experiments was the problem of measuring small changes in the LNAPL saturation with the γ-densitometer, given the inherent uncertainties of this measurement method. Special care was given to measuring the volume of mobilized LNAPL collected at the top of the column as a check against the densitometer results.

Also, the analysis of the densitometer data from the type 2 tests was complicated by the change in γ-coefficients caused by the addition of alcohol during the course of the run. Each time alcohol was added, the water/alcohol phase was circulated

through the test section for a sufficient duration to ensure that the alcohol concentration was uniform. The change in LNAPL γ-coefficient values indicated that a small amount of the alcohol was partitioning into the LNAPL phase. At higher alcohol concentrations, the samples of LNAPL used to measure the γ-coefficient values were apparently not representative of the residual LNAPL in the test section. This problem is addressed in the results discussion.

III. EXPERIMENTAL RESULTS AND DISCUSSION

The results for the type 1 test performed with 360-μm particles are shown in Figure 6. Figure 6A shows the initial water/alcohol saturation vs. vertical position in the test section. Figure 6B illustrates the measured saturation profiles for water/alcohol after the addition of LNAPL; the water/alcohol profile does not change appreciably here because the supply valve between the test section and the supply

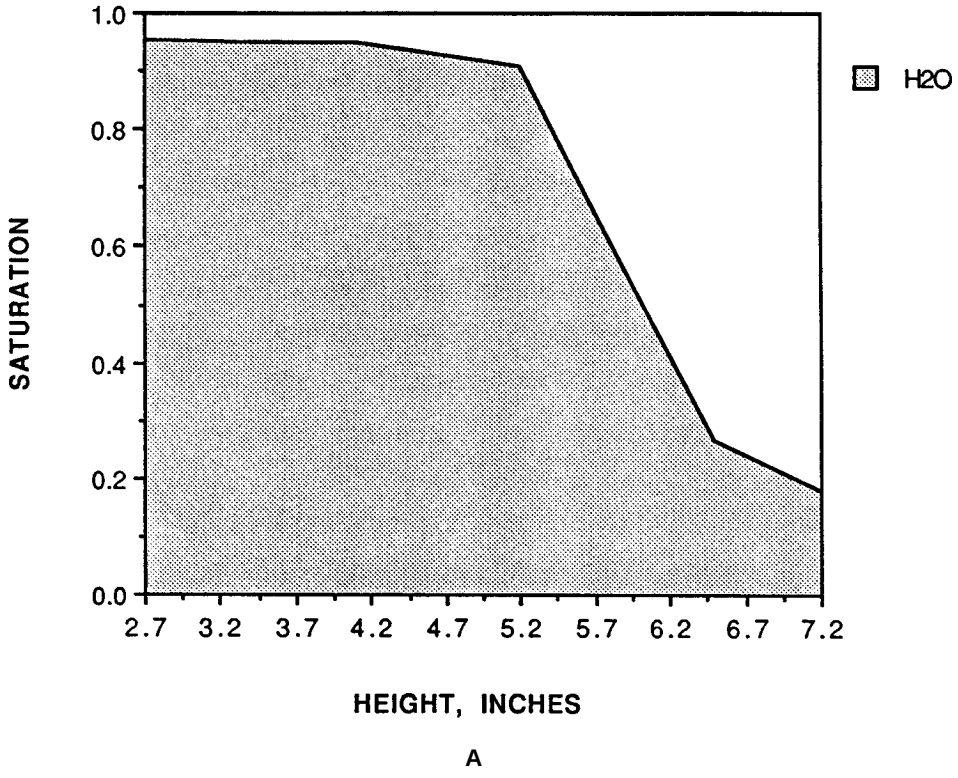

FIGURE 6. (A) Initial water saturation profile (360-μm particles with alcohol); (B) saturation profiles after LNAPL addition; (C) after first displacement by water; (D) after water level is lowered; (E) after second displacement by water.

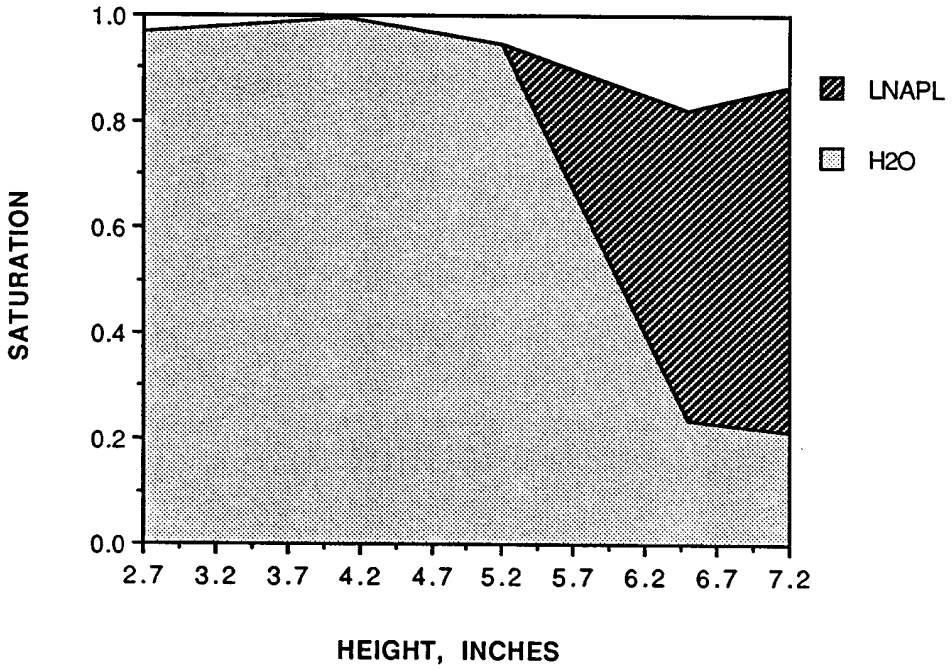

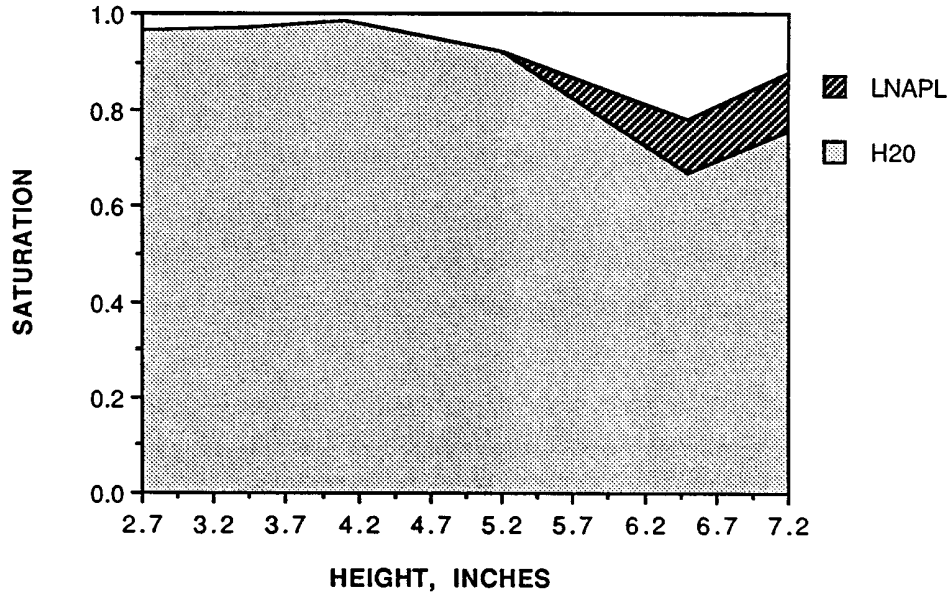

FIGURE 6B and C

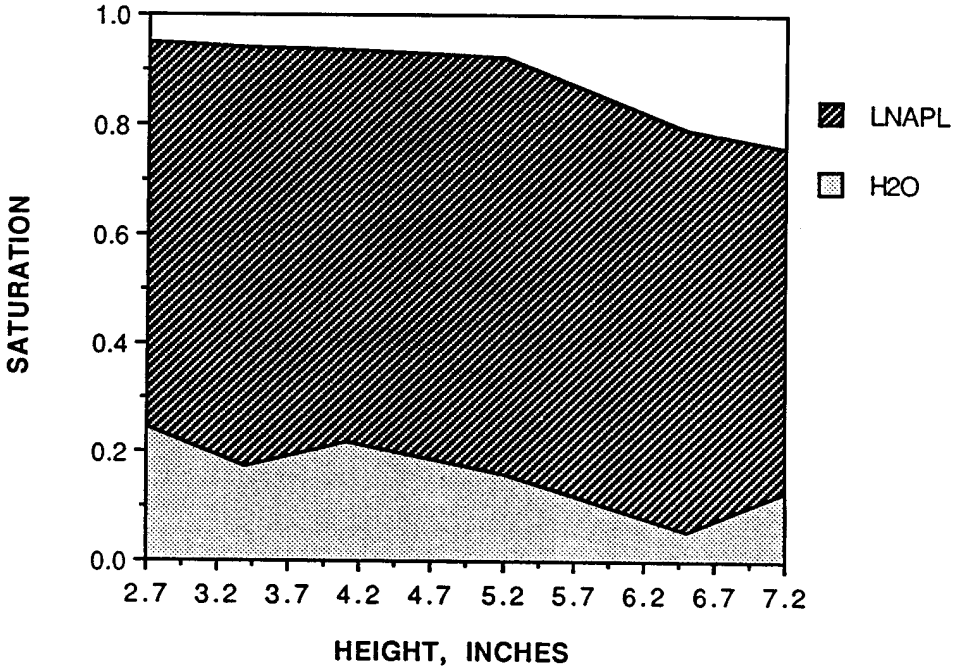

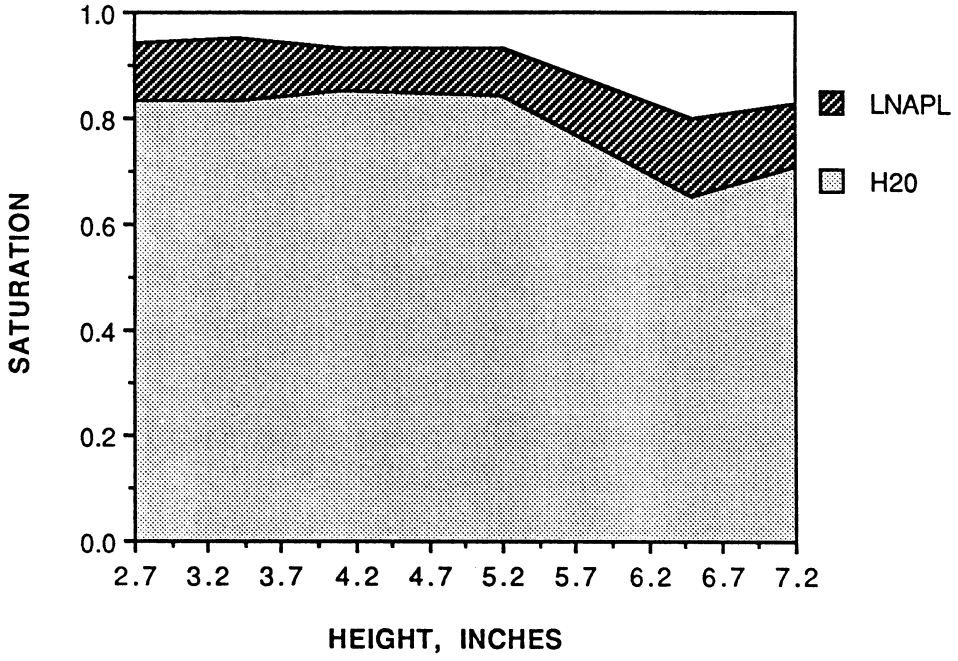

FIGURE 6D and E

tank is closed. The distribution of the trapped LNAPL after the first displacement by water is shown in Figure 6C. The residual saturation of the LNAPL at the two measurements nearest the top of the test section (at heights of 6.5 and 7.2 in.) were 11.3 and 11.9%, respectively. Figures 6D and E show the results from the second cycle of measurements. Because the water level was lowered sufficiently to allow the LNAPL to infiltrate the entire test section (Figure 6D), the residual saturation after the second displacement by water is quite uniform (Figure 6E), with the average value being 11.2%.

The results for the type 1 test performed with 1500-μm particles are shown in Figure 7. The effect of the particle diameter on the initial water profile can be noted in Figure 7A. Figures 7B to D show the saturation profiles at intermediate points in the run. Most importantly, the residual saturation distribution shown in Figure 7E is once again fairly uniform, but now the average value has dropped to 6.1%.

The measured interfacial tension between the water/alcohol and LNAPL phases for both of the type 1 runs was 8.0 dyn/cm. The corresponding Bond numbers

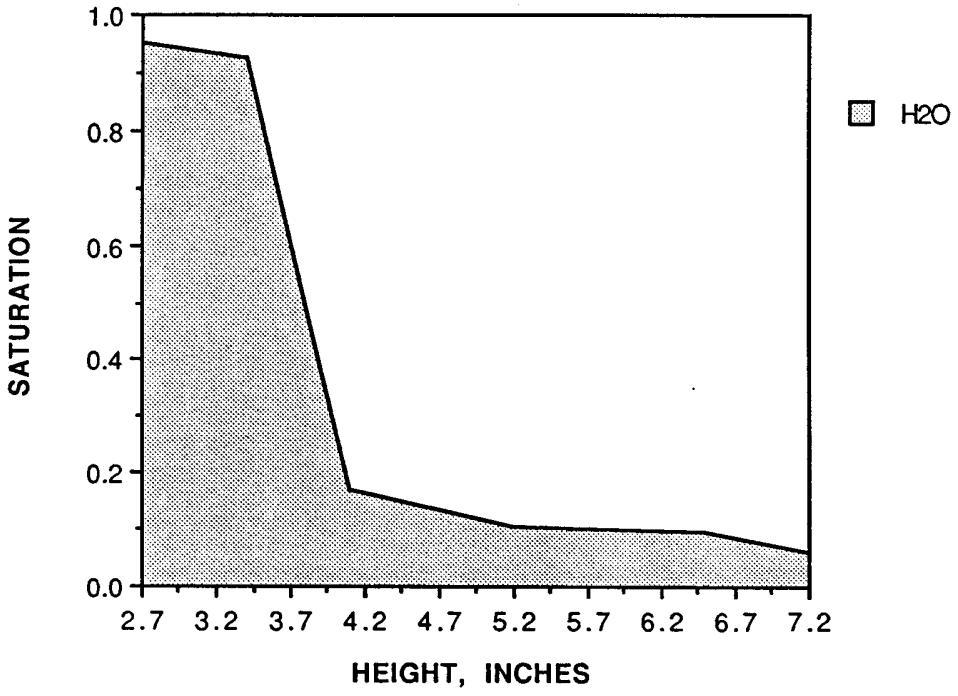

A

FIGURE 7. (A) Initial water saturation profile (1500-μm particles with alcohol); (B) saturation profiles after LNAPL addition; (C) after first displacement by water; (D) after water level is lowered; (E) after second displacement by water.

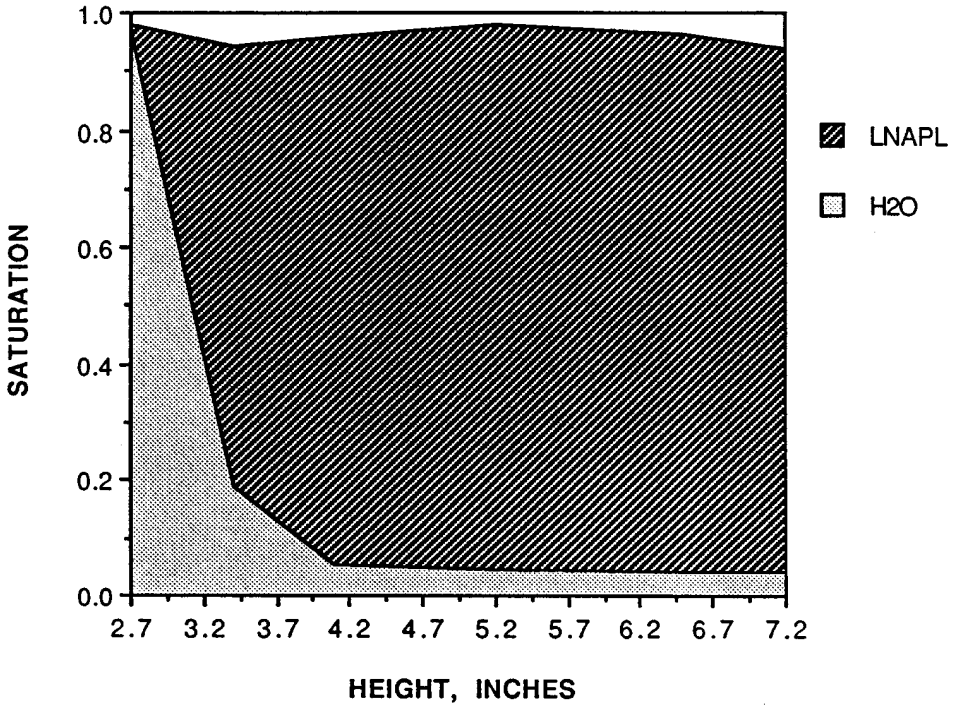

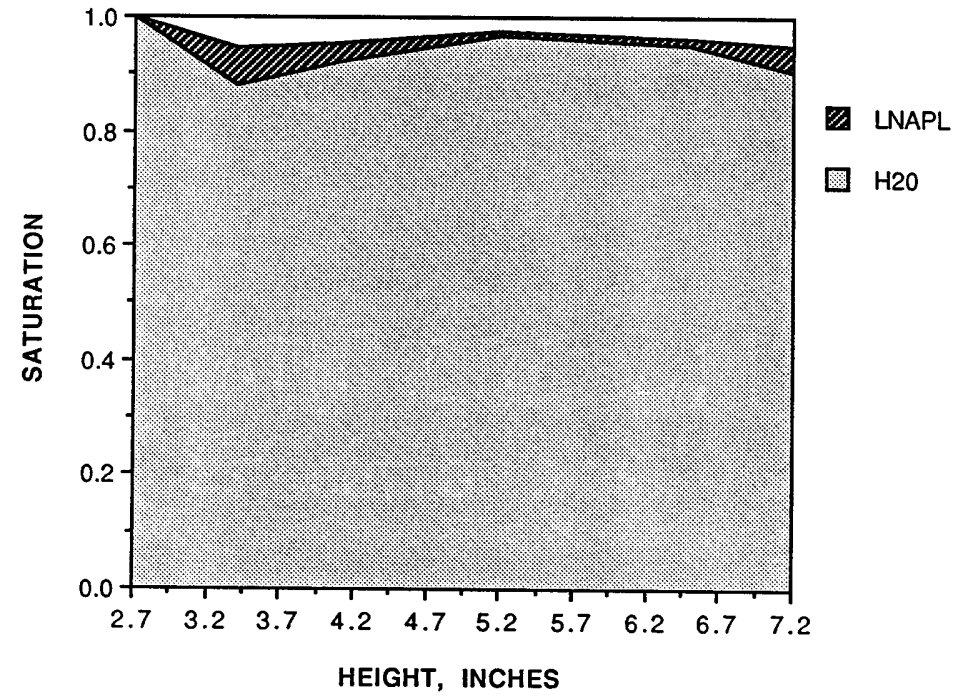

FIGURE 7B and C

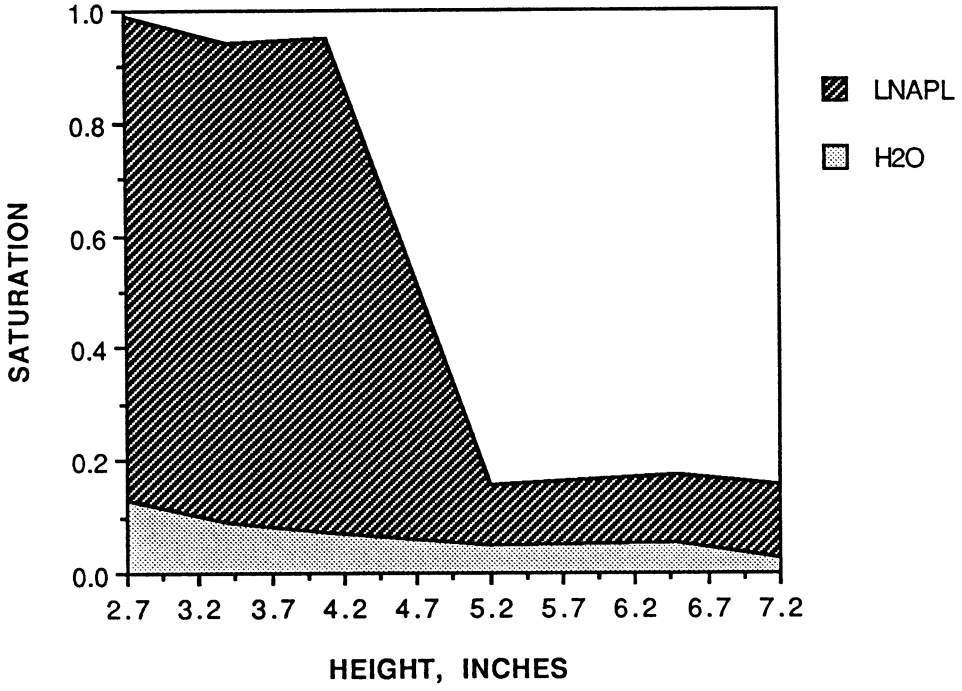

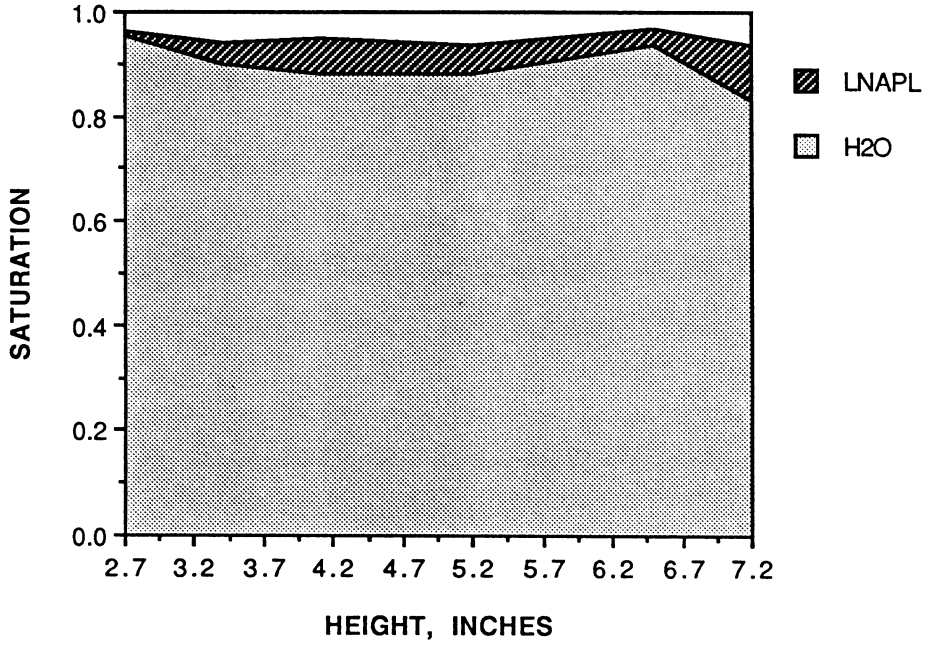

FIGURE 7D and E

(based on particle diameter) for the 360- and 1500-μm particles were 0.027 and 0.47, respectively.

The type 1 residual saturation results are plotted vs. Bond number along with the earlier results of Ryan and Dhir (1993) in Figure 8. The residual saturation values plotted in all cases are the average values after the second displacement by water. The excellent agreement with the earlier findings indicates that the effect of particle diameter and interfacial tension on the trapped LNAPL saturation may be correlated with the Bond number. It is thus reasonable to conclude that the sole effect of the alcohol addition on the trapping and mobilization phenomena in these experiments is due to the change in interfacial tension, and not changes in related fluid properties (e.g., contact angle).

The results of the type 2 test run with 1500-μm particles are shown in Figure 9. To begin the experiment, the type 1 procedure was run with water/NaBr only (no alcohol), corresponding to a Bond number of 0.12. The residual LNAPL saturation profile produced is plotted in Figure 9A. Subsequently, alcohol was added to the supply tank and circulated through the test section, producing a measured interfa-

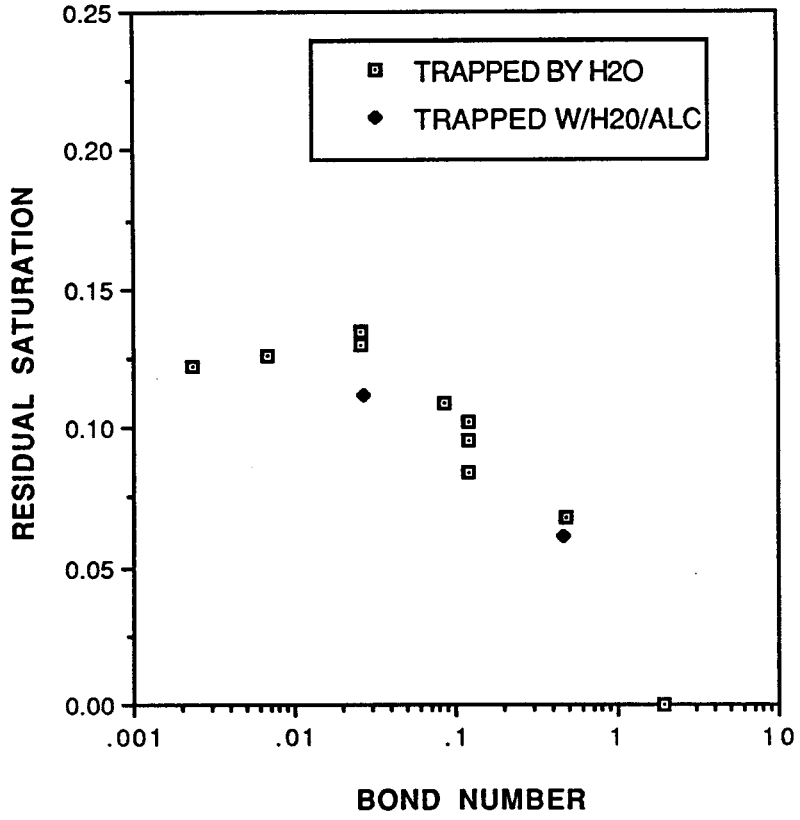

FIGURE 8. Comparison of trapped LNAPL saturation using water and water/alcohol as the displacing fluids.

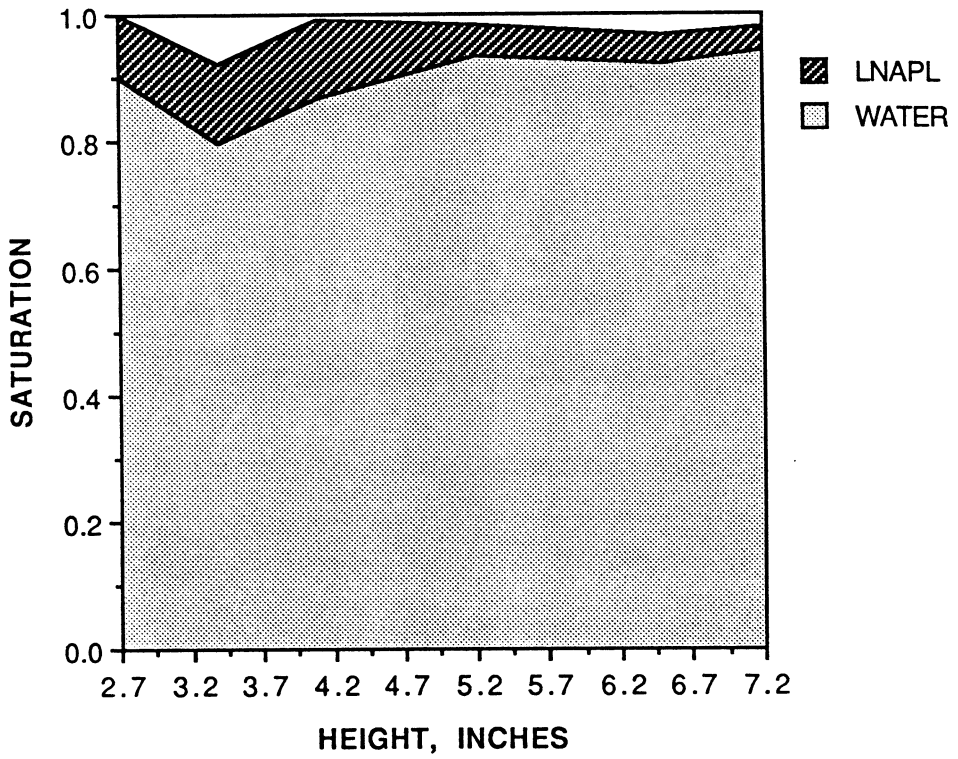

A

FIGURE 9. Saturation profiles (A) after displacement by water — 1500μm particles (Bo = 0.12); (B) after mobilization by water/alcohol (Bo = 0.37).

cial tension of 11.7 dyn/cm (and a Bond number of 0.37). No measurable amount of LNAPL escaped from the test section. The measured saturations from the densitometer data are shown in Figure 9B. There is some indication of a slight upward redistribution of LNAPL within the test section; the LNAPL volumes in the test section calculated from integrating the saturation data of 19.8 ml (corresponding to Figure 9A) and 20.4 ml (corresponding to Figure 9B) were consistent with the lack of mobilized LNAPL observed. It should be noted that the values of the γ-counts measured through the test section varied significantly for these two cases, due to the change in the γ-coefficients. The consistency of the saturation profiles shown in Figures 9A and B provide confidence in the experimental procedure.

Subsequent alcohol addition yielded an interfacial tension of 5.8 dyn/cm and a Bond number of 0.63, and began producing a measurable amount of free LNAPL at the top of the column. The free LNAPL was collected and had a measured

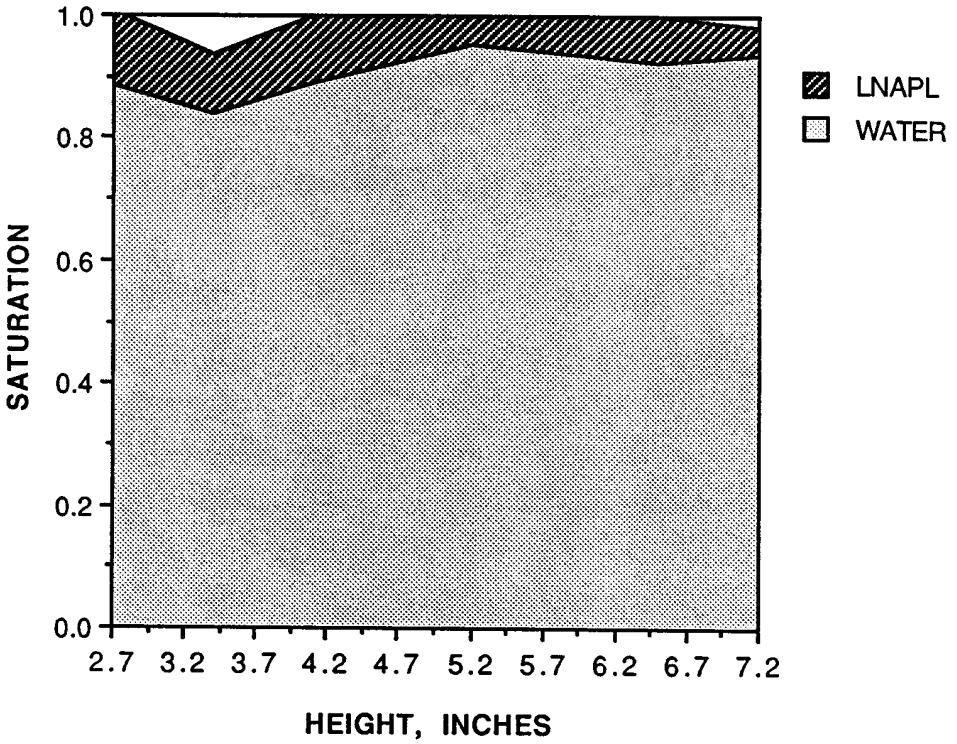

FIGURE 9B

volume of 4 ml. However, the densitometer data from this portion of the experiment did not give saturations consistent with the amount of LNAPL known to be in the test section. Because the 4 ml of LNAPL collected was not a sufficient volume to measure the γ-coefficients, some fresh LNAPL was allowed to equilibrate with some of the water/alcohol solution taken from the supply tank, and used for γ-coefficient and interfacial tension measurement. (This procedure was also used to produce the results given in Figure 9B and gave consistent values, as noted above.) Apparently, this procedure does not sufficiently duplicate the state of the LNAPL in the test section at higher alcohol concentrations. However, knowing the volume of mobilized LNAPL allowed an average change in residual saturation in the test section to be calculated.

The results for 3000-μm particles are shown in Figure 10. Figure 10A shows the residual saturation profile produced by trapping with water/NaBr, corresponding to a Bond number of 0.48. The average residual LNAPL saturation measured was 2.99%. The amount of LNAPL retained in the test section based on integrating the saturation profile (9.0 ml) agrees well with the value based on the difference between the amount added and the amount displaced (11 ml).

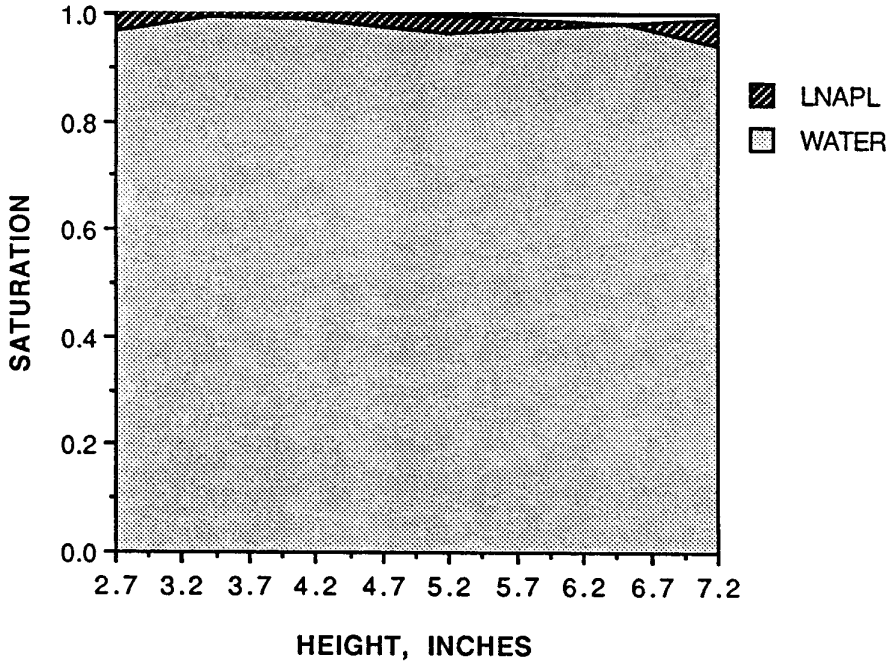

A

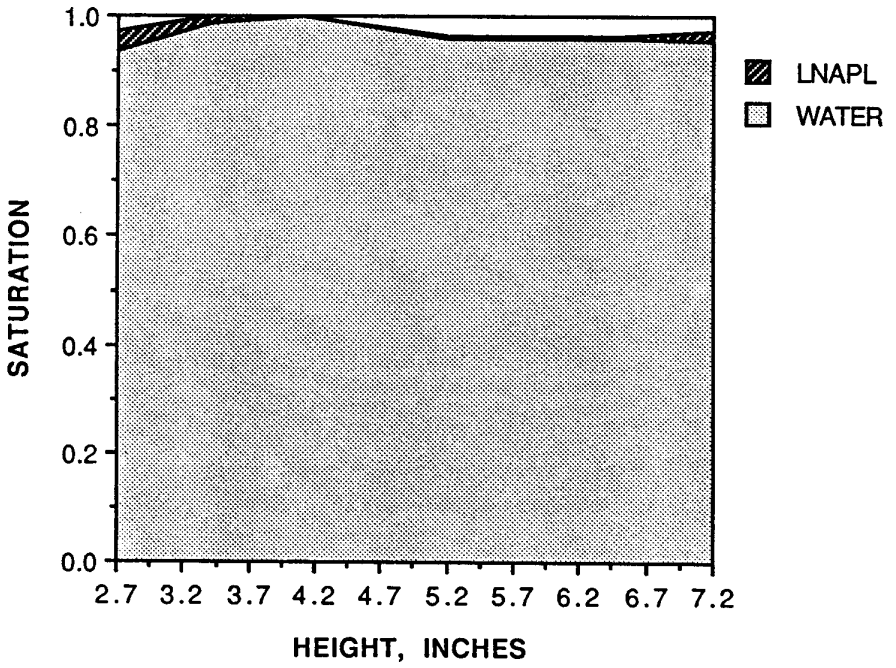

B

FIGURE 10. Saturation profiles (A) after displacement by water — 3000-µm particles (Bo = 0.48); (B) after mobilization by water/alcohol (Bo = 1.11).

After sufficient alcohol was added to decrease the interfacial tension to 15.9 dyn/cm (and increase the Bond number to 1.11), the saturation profile was measured and is shown in Figure 10B. During this alcohol addition, 9 ml of LNAPL was mobilized and collected at the top of the column, indicating that only 2 ml of LNAPL remained in the test section. This compares well with the value of 3.65 ml calculated from the measured saturation values; the corresponding average residual saturation was 1.3%.

Subsequent alcohol addition yielded an interfacial tension of 9.1 dyn/cm and a Bond number of 1.75. Traces of mobilized LNAPL (approximately 1 ml) were observed; the lack of significant amounts was expected because the results of Figure 10B indicate that there was little LNAPL left in the test section.

Figure 11 summarizes the results from the mobilization experiments. The saturation values corresponding to the highest Bond number for each run are based on the amount of LNAPL mobilized during the last alcohol addition; the values from the densitometer measurements were not used due to the measurement problem at high alcohol concentrations mentioned previously. It can be seen that the onset of mobilization of the trapped LNAPL occurs at a similar Bond number for both runs.

A better overall view of the relationship between LNAPL residual saturation and Bond number is shown in Figure 12, which summarizes all of the experiments

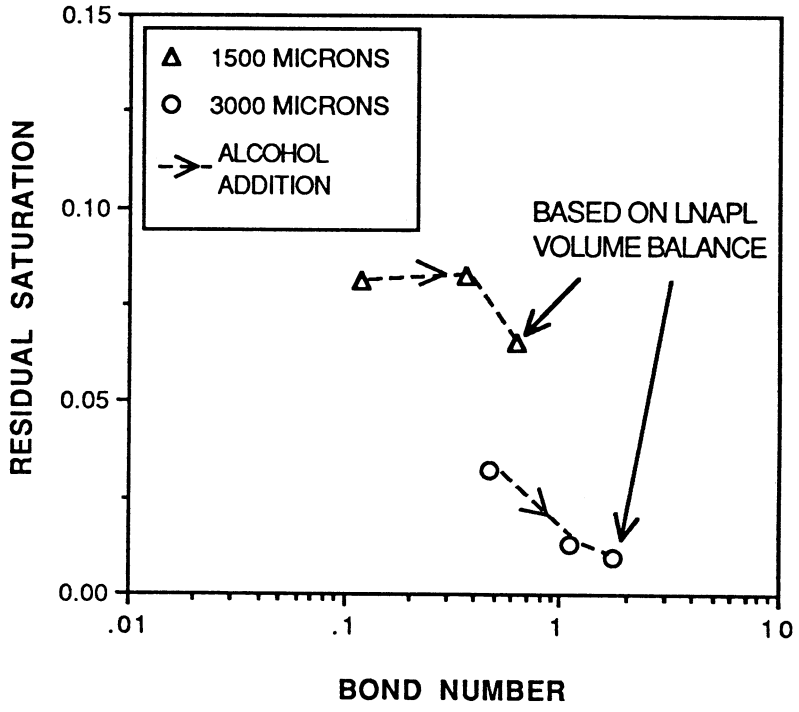

FIGURE 11. Effect of alcohol addition on mobilization of trapped LNAPL.

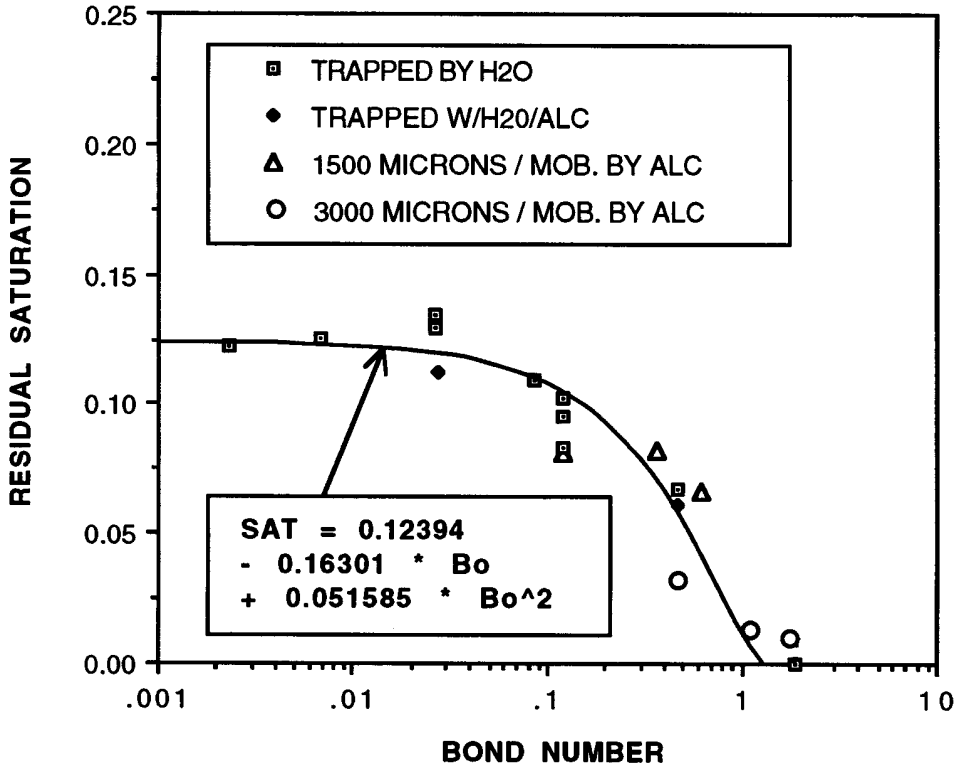

FIGURE 12. Summary of all runs vs. bond number.

performed with different particle diameters and interfacial tensions. It is clear that as the Bond number approaches one (either through larger particle size or reduced interfacial tension), the residual LNAPL saturation drops to negligible values. This is true for both trapping experiments, where continuous LNAPL is slowly displaced by water (or water/alcohol), and for mobilization experiments (i.e., type 2 experiments), where discontinuous LNAPL ganglia are displaced by a reduction in interfacial tension.

The similarity in the saturation/Bond number relationship for trapping and mobilization experiments is consistent with the hypothesis that most of the trapped LNAPL is contained in single-pore globules (or singlets). If a significant number of larger globules were created during the trapping process, they would be mobilized first as interfacial tension decreases because the net buoyancy force is proportional to ganglion length. The large, mobilized globules would tend to break up into smaller pieces and thus require a further decrease in interfacial tension to remobilize. Thus, a hysteresis between the trapping and mobilization curves would be expected. The lack of observed hysteresis suggests that the trapping of single-pore globules by "snap-off" is the dominant mechanism.

An empirical correlation was developed between LNAPL residual saturation and Bond number and is also shown in Figure 12. The correlation is quadratic in form and may be used for Bond numbers between 0.001 and 1.2:

$$SAT = 0.12394 - 0.16301\ Bo + 0.051585\ Bo^2 \quad (5)$$

It should be stressed that this correlation is only valid for upward LNAPL displacement in an unconsolidated porous medium that is "water wet," that is, the particle surfaces were initially wetted with water prior to the invasion by LNAPL. However, as previously noted, these conditions are generally satisfied for aquifer materials in the vicinity of the water table, so the correlation should be applicable to field situations.

IV. COMPARISON WITH PUBLISHED RESULTS

Comparison of these results to previous water-flooding experiments by petroleum engineers indicate a similarity between the effects of hydrostatic pressure gradients and viscous pressure gradients on residual LNAPL saturation. Observations by Wardlaw and McKellar (1985) indicate that larger oil ganglia break up after mobilization, so that there is no significant oil recovery until the capillary number is high enough to mobilize single-pore blobs, or singlets. According to their experimental results, a capillary number of 1E-3 is required for singlet mobilization. Equating the hydrostatic pressure gradient with the viscous pressure gradient at this critical capillary number, a critical Bond number of 1.6 (based on particle diameter) for LNAPL mobilization is predicted (Ryan and Dhir, 1993). This prediction is in good agreement with the results shown in Figures 11 and 12.

In order to compare Bond numbers based on particle diameter with those based on permeability, a relationship between these two parameters must be known. An appropriate relationship is an empirical correlation given by Bear (1972):

$$k = 6.17E\text{-}4\ D_p^2 \quad (6)$$

Another alternative is the relationship by Fair and Hatch (1933):

$$k = D_p^2 \varepsilon^3 / 180(1-\varepsilon)^2 \quad (7)$$

For an average porosity of 39%, this reduces to:

$$k = 8.86E\text{-}4\ D_p^2 \quad (8)$$

Measurements of permeability for the 360-μm particles used in these experiments gave values between the predictions of the Bear (1972) and Fair and Hatch (1933)

relationships. Taking an average, a factor of 7.5E-4 is reasonable to convert between the different Bond number definitions. The data presented in Figure 11 indicate that mobilization of entrapped LNAPL begins at a Bond number of 0.4; multiplying by the conversion factor gives a Bond number based on permeability of 3.0E-4. This value can be compared with other published data. The corresponding mobility number would be similar in magnitude because the capillary number in these experiments is negligible and the ratio of relative permeability to porosity is fairly close to one.

Boyd and Farley (1992) assessed the effectiveness of alcohol flooding for the removal of residual TCE from glass bead packs and South Carolina soil. Because their experiments were run in both horizontal and vertical orientations, the effect of buoyancy was accounted for by correlating their data with respect to the mobility number. The results showed that mobilization of entrapped TCE began at a mobility number of 1E-4, and complete removal was achieved at 1E-2.

More recently, Duggan *et al.* (1994) studied mobilization of gasoline range hydrocarbons using a variety of surfactants to reduce the interfacial tension. Experiments were run in a vertical column using a concrete sand from a Connecticut stratified deposit contaminated with *m*-xylene. The results suggested that mobilization of the trapped contaminant begins when the sum of the capillary and Bond numbers exceeds 2.0E-4.

Lenhard *et al.* (1993) presented data for *in situ* LNAPL residual saturation values following vertical water table displacements in a soil described as 97.5% sand, 0.8% silt, and 1.7% clay. Distribution of the liquid phases was measured with a γ-densitometer. The data show a significant effect of the initial water saturation on the LNAPL residual saturation. The measured residual LNAPL values ranged from 5 to 32%, which corresponded to initial water saturation values (prior to LNAPL addition) of approximately 100 to 30%. This wide range of residual LNAPL saturations was not seen in the results presented here or previously in Ryan and Dhir (1993), with one exception. A sample of particles was inadvertently exposed to moisture prior to testing, causing a possible spatial variation in contact angle that may have led to trapping by "fingering" of the invading water phase. Trapping by fingering may be an important mechanism in soils that are not homogeneous.

Data were presented by Dawson (1992) for the displacement of TCE (a NAPL denser than water) in Borden sand by water floods at various velocities. Most of the data presented were for upward displacement of TCE, where the net buoyancy force acts opposite to the direction of displacement. However, some data were presented for downward displacement of TCE at low capillary numbers; values of average residual TCE from 14.5 to 18.4% were measured. These values are a few percentage points higher than the values presented here at low Bond number (see Figure 12).

Simulations by Dawson (1992) using the ganglion mobilization model cited earlier were presented for residual saturations following vertical displacements of

a typical LNAPL by water. The results suggest a critical Bond number that is approximately three orders of magnitude less than the values given here. The discrepancy would appear to be explained by the long ganglion lengths (tens of centimeters) used in the simulations. The value of critical Bond number found in these experiments and the lack of hysteresis between the trapping and mobilization curves support the hypothesis that most of the entrapped ganglia are in the form of singlets, or single-pore blobs. A more realistic model for ganglion lengths is probably necessary for better simulation of trapping and mobilization of NAPLs in the saturated zone.

V. CONCLUSIONS

The results presented here combined with the earlier findings of Ryan and Dhir (1993) were used to establish a correlation between LNAPL residual saturation and Bond number. The correlation is valid for LNAPLs trapped by upward water table displacements in water-wet media, which should be typical of natural conditions near the water table. The correlation can be used to estimate the amount of LNAPL trapped in the saturated zone by water table variations due to recharge events, or to estimate the interfacial tension reduction required to mobilize entrapped contaminants.

The data presented here show a fairly uniform vertical distribution of the residual LNAPL. Other studies have shown variations dependent on initial water saturation. These differences might be explained by spatial variations of contact angle within the medium; more experimental work is required to resolve these differences.

There appears to be general agreement among this study and others regarding the Bond number required to initiate mobilization of entrapped LNAPL ganglia. This "critical Bond number" appears to lie between 1E-4 and 3E-4 (using a Bond number based on permeability). The similarity between the saturation-Bond number relationship in the trapping and mobilization experiments supports the hypothesis that most of the LNAPL is entrapped in single-pore blobs by the snap-off mechanism. This information can be used to improve modeling efforts for predicting LNAPL residual saturation.

REFERENCES

Adamson, A. W. 1967. *Physical Chemistry of Surfaces.* New York, Wiley-Interscience.

Bear, J. 1972. *Dynamics of Fluids in Porous Media.* New York, Elsevier.

Boyd, G. R. and Farley, K. J. 1992. NAPL removal from groundwater by alcohol flooding: laboratory studies and applications. In: *Hydrocarbon Contaminated Soils and Groundwater,* Vol. 2. (Calabrese, E. J. and Kostecki, P. T., Eds.) Lewis Publishers.

Dawson, H. E. 1992. Entrapment and Mobilization of Residual Halogenated Organic Liquids in Saturated Aquifer Material. Palo Alto, CA, Ph.D. thesis, Stanford University.

Duggan, J. W., Bruell, C. J., and Ryan, D. K. 1994. In situ emulsification and mobilization of gasoline range hydrocarbons using surfactants. *J. Soil Contam.* **3**.

Fair and Hatch. 1993. *J. AWWA.* p. 1551.

Hoag, G. E., Marley, M. C., Cliff, B. L., and Nangeroni, P. 1991. Soil vapor extraction research developments. In: *Hydrocarbon Contaminated Soils and Groundwater*, Vol. 1. (Kostecki, P. T. and Calabrese, E. J., Eds.) Lewis Publishers.

Lenhard, R. J. and Parker, J. C. 1988. Experimental validation of extending two-phase relations to three-fluid phase systems for monotonic drainage paths. *Water Resour. Res.* **24**.

Lenhard, R. J., Parker, J. C., and Kaluarachchi, J. J. 1989. A model for hysteretic constitutive relations governing multiphase flow. III. Refinements and numerical simulations. *Water Resour. Res.* **25.**

Lenhard, R. J., Johnson, T. G., and Parker, J. C. 1993. Experimental observations of nonaqueous-phase liquid subsurface movement. *J. Contam. Hydrol.* **12.**

Leverett, M. C. 1941. Capillary behavior in porous solids. *Trans. Am. Inst. Mineral. Eng.* **142.**

Parker, J. C. and Lenhard, R. J. 1987. A model for hysteretic constitutive relations governing multiphase flow. I. Saturation-pressure relations. *Water Resour. Res.* **23.**

Ryan, R. G. and Dhir, V. K. 1993. The effect of soil-particle size on hydrocarbon entrapment near a dynamic water table. *J. Soil Contam.* **2.**

Ryan, R. G. 1994. The Effect of Soil Particle Size and Interfacial Tension on Hydrocarbon Entrapment Near a Dynamic Water Table. Los Angeles, Ph.D. thesis, University of California.

Wardlaw, N. C. and McKellar, M. 1985. Oil blob populations and mobilization of trapped oil in unconsolidated packs. *Can. J. Chem. Eng.* **63.**